Available online at www.sciencedirect.com

ScienceDirect

Geochimica et Cosmochimica Acta 247 (2019) 207–219

Geochimica et Cosmochimica Acta

www.elsevier.com/locate/gca

Amino acid enantiomers in old and young dissolved organic matter: Implications for a microbial nitrogen pump

Taylor A.B. Broek [a,b,*,1], Amy L. Bour [a,1], Hope L. Ianiri [a], Thomas P. Guilderson [a,b], Matthew D. McCarthy [a]

[a] University of California, Santa Cruz, Ocean Sciences Department, 1156 High Street, Santa Cruz, CA, USA
[b] Lawrence Livermore National Laboratory, Center for Accelerator Mass Spectrometry, 700 East Avenue, B-1888 Livermore, CA, USA

Received 12 January 2018; accepted in revised form 21 December 2018; available online 4 January 2019

Abstract

Dissolved organic nitrogen (DON) represents the largest reservoir of fixed N in the surface ocean and a significant portion accumulates in the deep sea, where it can persist for millennial time scales. However, like the dissolved organic carbon (DOC) pool, the origin and composition of long-lived, refractory DON remains largely unknown. In recent years, the "microbial carbon pump" hypothesis has emerged from abundant evidence showing that microbial processes are primarily responsible for refractory DOC accumulation. However, a similar mechanism for DON has rarely been investigated. In the study of DON, spectroscopic evidence has indicated a primarily amide composition, implying a dominant contribution from peptides. Therefore, if an analogous "microbial nitrogen pump" controls refractory DON accumulation, the amino acid component should bear increasing signatures of microbial origin with increasing age. Here we investigate the microbial sequestration of N via the production of refractory DON, for the first time considering together DOM $\Delta^{14}C$ with amino acid (AA) molar abundance (Mol%) and D/L ratio (as a tracer for prokaryotic input). Measurements were made on a unique set of high and low molecular weight (HMW, LMW) DOM isolates with ^{14}C ages and chemical compositions generally consistent with semi-labile and refractory DOM respectively. The samples were collected in the North Pacific Subtropical Gyre where deep waters contain some of the oldest DOC in the world ocean. We observe higher D/L ratios in older, LMW DOM isolates for almost all analyzed AAs. Using mass spectral data, we also quantify three D-AAs in all samples (D-valine, D-phenylalanine, and D-leucine), which have not previously been confirmed in ocean DOM. These newly identified D-AAs are concentrated in the LMW refractory DOM fraction and have oceanographically consistent depth profiles. Our results suggest that several novel D-AA subgroupings may be unique tracers for different prokaryotic source processes. D-alanine appears to have largely independent cycling from the other D-AAs with a connection to the production of HMW DON, which we hypothesize is linked to water column peptidoglycan. In contrast, D-leucine, D-valine, and D-phenylalanine appear to be most strongly related to the production of LMW DON. Trends in both the HMW and LMW fractions suggest a linkage to sinking particles and local microbial transformations, implying that LMW DON has a direct biological source rather than originating from successive microbial reprocessing of HMW DON. Taken together, our observations are consistent with the dominant production of refractory LMW DON by prokaryotic organisms and suggests that different AA sub-groupings that can be used to track different processes within the DON pool.

Keywords: Amino Acid Enantiomers; Dissolved Organic Matter; Molecular Weight

* Corresponding author.
E-mail address: tborrius@ucsc.edu (T.A.B. Broek).
[1] Taylor Broek and Amy Bour contributed equally to this work.

https://doi.org/10.1016/j.gca.2018.12.037
0016-7037/

1. INTRODUCTION

Marine dissolved organic matter (DOM) exerts a critical influence on climate, the microbial food web, and ocean nutrient regimes. This carbon (C) reservoir is comparable in size to atmospheric CO_2, and equivalent to more than five years of global net primary production (Woodward, 2007; Hansell et al., 2009). Ocean DOM likely originates almost entirely from marine primary production (Hansell et al., 2009), however only a small fraction is identifiable as common biomolecules (Benner and Amon, 2015). Despite major advances in techniques to study the DOM pool, most remains structurally unidentified at the molecular level (Repeta, 2014). This is particularly true in the subsurface ocean, where DOM is characterized by average radiocarbon (^{14}C) ages of 4000–6000 years (Williams and Druffel, 1987), and is dominated by low molecular weight compounds (Benner and Amon, 2015) with an enormous diversity of molecular structures (Koch et al., 2005).

Many explanations for the preservation of long-lived, or refractory DOM have been proposed, including non-marine origin, abiotic condensation reactions, microenvironments, particle interactions, photochemistry, and hydrothermal sources (Hedges, 1992; Benner and Ziegler, 1999; Nagata and Kirchman, 1999; Hedges et al., 2000; Kirchman, 2004; Eglinton and Repeta, 2006; Ziolkowski and Druffel, 2010; McCarthy et al., 2010; Arrieta et al., 2015). Recent work, however, has increasingly focused on microbial control of DOM cycling (Kaiser and Benner, 2008; Yamaguchi and McCarthy, 2018), showing that refractory DOM compounds are characterized by novel molecular structures and/or low concentrations that cause metabolic costs to outweigh the benefits of biological utilization (Hertkorn et al., 2013; Dittmar, 2014; Arrieta et al., 2015). Bacteria not only degrade and metabolize OM, but can significantly contribute material to the bulk OM pool, for example: in DOM, marine snow, and sediments in lakes and oceans (Simon et al., 1990; Gweon and Fisher, 1992; Lehmann et al., 2002; Tremblay and Benner, 2006; McCarthy et al., 2007; Kaiser and Benner, 2008; Alkhatib et al., 2012; Carstens and Schubert, 2012; Niggemann et al., 2018). It has been clearly shown in laboratory experiments that heterotrophic microbes can produce refractory DOM from simple organic molecules and common biopolymers, characterized by increased structural complexity and decreased nutrient and energy content, (Ogawa, 2001; Benner and Amon, 2015; Lechtenfeld et al., 2015). The production of refractory DOM and associated carbon sequestration by bacteria, archaea, and viruses has, in recent years, been termed the "microbial carbon pump" (MCP; Jiao et al., 2010). The MCP idea represents a synthesis of a large number of prior studies which have examined the importance of microbial source and processes in the production of refractory molecules (Benner and Amon, 2015). Multiple specific mechanisms have been hypothesized as potential explanations for the formation of refractory DOM via an MCP, including the diversity of bacterial metabolic pathways, promiscuous exoenzymes, structural modification, and selective remineralization associated with microbial degradation (Jiao et al., 2010).

In contrast, the production of refractory DON and associated N sequestration via a microbial nitrogen pump (MNP; Yamaguchi and McCarthy, 2018) in many ways presents a greater puzzle. As with the more commonly explored MCP, this idea represents a shorthand to synthesize multiple past studies aimed at understanding bacterial sources and transformations. However, in contrast to the enormous complexity of DOC chemical functionality, solid state ^{15}N NMR analysis has indicated that DON is composed almost entirely of amide nitrogen (McCarthy et al., 1997; Mao et al., 2012; Sipler and Bronk, 2014). This observation strongly suggests that a very limited range of common biochemical structures, such as peptides and N-acetyl amino polysaccharides, are the dominant biomolecular components at all ocean depths (McCarthy et al., 1997; Aluwihare et al., 2005). These compound classes are among the most labile of all biochemicals (Cowie and Hedges, 1992; Jørgensen et al., 2014), and the amide linkage itself indicates relatively intact biopolymers (McCarthy et al., 1997). Nevertheless, deep ocean $\Delta^{14}C$ data suggests this same material survives over multiple ocean mixing cycles (Loh et al., 2004), while spectroscopic data has indicated rapidly diminishing amino sugar contribution in the subsurface ocean (Aluwihare et al., 2005). Together, these observations have suggested that proteinaceous material is the dominant subsurface compound class, even in refractory DON (McCarthy et al., 1997; McCarthy and Bronk, 2008). At the same time, primary production remains N-limited in the subtropical gyres despite the presence of micro-molar concentrations of DON (Moore et al., 2013; Sipler and Bronk, 2014). Taken together these observations present a conundrum: although both phytoplankton and heterotrophic bacteria can use DON (Bronk et al., 2007; Sipler and Bronk, 2014), and spectroscopic properties suggest that it is dominated by common, labile biochemical classes, relatively refractory DON is apparently produced in surface waters and persists for millennia in the deep ocean.

If the formation of refractory DON is in fact directly linked to microbial source, then an MNP presumably depends largely on transformations of the combined amino acid (AA) fraction of the DOM pool (Yamaguchi and McCarthy, 2018). AAs are the largest identifiable component of DON and therefore represent the main biochemical class which could be used to investigate the microbial production of refractory DON at the molecular level (Eglinton and Repeta, 2006; McCarthy and Bronk, 2008). The structural diversity and differential utilization of AAs provides a wealth of molecular tracer potential. Molar percentage metrics have long been used as powerful indicators of relative degradation state and recalcitrance (Dauwe et al., 1999; Yamashita and Tanoue, 2003; McCarthy et al., 2004; Lechtenfeld et al., 2014; Lechtenfeld et al., 2015). However, for investigating direct bacterial source, the D-enantiomer of AAs (D-AAs) represent arguably the most powerful molecular tracer. The synthesis and incorporation of D-AAs into biochemicals is confined almost exclusively to prokaryotic organisms, making D-AAs among the few unambiguous proxies for bacterially derived molecules in the modern ocean (McCarthy et al., 1998; Kaiser and Benner, 2008; Radkov and Moe, 2014).

Finally, a growing body of recent research has shown that molecular size (or molecular weight) of dissolved organic matter is directly associated with both its reactivity and composition reviewed by Benner and Amon (2015), and is also directly correlated with DOM ^{14}C age distributions (Walker et al., 2011; Walker et al., 2014; Walker et al., 2016). Specifically, observations of bulk molecular and isotopic properties suggest DOM exists in a continuum of size, age, and biological reactivity: high molecular weight (HMW) DOM is dominated by more freshly produced, semi-labile material, while lower molecular weight (LMW) DOM has far older ^{14}C ages, contains fewer identifiable biomolecules, and is generally more biologically refractory (Walker and McCarthy, 2012; Benner and Amon, 2015; Walker et al., 2016; Broek et al., 2017). These sized based trends combined with the MCP conceptual framework suggest that successive microbial utilization and reprocessing corresponds with the production of smaller and increasingly refractory compounds. If microbial processes are primarily responsible for refractory DON formation, one might therefore expect a direct relationship between DOM molecular weight, ^{14}C age and abundance of bacterial tracers.

Here we directly examine these ideas using a novel approach coupling $\Delta^{14}C$ data with AA D/L enantiomeric ratios and relative AA molar abundance (AA-Mol%) measurements of separately isolated HMW and LMW DOM fractions from the North Pacific Subtropical Gyre. This site is the largest ocean biome on earth, and has deep waters which represent the endmember of overturning ocean circulation and contain the ocean's oldest DOM. Our main goal is to test the hypothesis that a linkage of D-AA with $\Delta^{14}C$ age would implicate bacteria as the direct sources for the progressive accumulation of refractory DON in the ocean. In addition, our large-volume DOM isolations allowed application of GC–MS analyses to identify an expanded suite of novel D-AAs not previously reported in marine DOM, but highly concentrated in the more refractory, LMW fraction. Together our results indicate that D-AA tracer potential in DOM is substantially greater than previously recognized. While our data strongly supports the basic MNP idea, it also suggests some surprising conclusions about the link between bacterial sourced refractory DON and molecular weight in the ocean.

2. EXPERIMENTAL METHODS

2.1. Water sampling

Our analyses were conducted on subsamples of the high molecular weight ultrafiltered DOM (HMW UDOM) and low molecular weight solid phase extracted DOM (LMW SPE-DOM) fractions previously described in Broek et al. (2017). These DOM samples were collected using a sequential sampling approach in which HMW DOM was first concentrated using a large-volume tangential-flow ultrafiltration (UF) system, at high concentration factor (CF; ~1000). LMW DOM which permeated the UF system was then isolated by solid-phase extraction (SPE). Broek et al. (2017) describe extensive testing and comparison of LMW isolates, showing that the isolated LMW material has isotopic ratios and bulk properties representative of total LMW DON (see additional discussion in Section 4.1). Sampling was conducted at the Hawaii Ocean Time Series Station ALOHA (A Long-Term Oligotrophic Habitat Assessment; 22°45′N, 158° 00′W) aboard the R/V Kilo Moana cruises KM1418 (late Summer 2014) and KM1506 (Spring 2015). A full description of the sampling protocol and materials is presented in the appendix (appendix section 1.1) and is detailed elsewhere (Broek et al., 2017). The HMW ultra-filtered material represents $17 \pm 1\%$ and $9 \pm 2\%$ of total DOC in the surface (7.5 m) and subsurface (400–2500 m) respectively, and the LMW SPE-DOM fraction represents $23 \pm 2\%$ of the remaining LMW DOC in the surface and $32 \pm 2\%$ in the subsurface. A thorough discussion of the extraction efficiency of the combined UF/SPE is presented in Broek et al. (2017).

2.2. Sample preparation

Liquid-state acid hydrolysis was used to liberate individual AAs following the recommendations for reduction of racemization blanks (Kaiser and Benner, 2005). A 3.75 mgC subsample of HMW UDOM or LMW SPE-DOM material, representing approximately 20 L (surface) and 100 L (mesopelagic and deep) of seawater for HMW UDOM, and 20–30 L of seawater for LMW SPE-DOM, were weighed into combusted vials (450 °C/5 hrs). 3 mL of 6 M HCl was added, vials were purged with N_2 and heated to 110 °C for 20 hr. Acid hydrolysis completely deaminates asparagine (Asn) to aspartic acid (Asp) and glutamine (Gln) to glutamic acid (Glu), therefore the abbreviations Asx and Glx are used throughout to denote the combination of Asp/Asn and Gln/Glu respectively. HCl was removed under a stream of N_2, and the hydrolysates were re-dissolved in 1 mL of 0.1 M HCl. Hydrolysates were then purified using cation-exchange chromatography (Bio-Rad AG50W-X8, 200–400 mesh), following the methods of Takano et al. (2010). The ammonium hydroxide in eluted column samples was removed using the Jouan centrifugal evaporator (Societe Jouan, Saint-Herblain, France) at a chamber temperature of 55 °C, and amino acids were then protonated by dissolving in 1 mL 0.1 M HCl. Trifluoroacetyl isopropyl ester derivatives were prepared following the general protocol of Silfer et al. (1991), with modifications discussed in Décima et al. (2017). AAs were further purified by solvent extraction followed by re-acetylation, as described by Décima et al. (2013) and samples were stored at −20 °C for up to two weeks before analysis. Immediately before chromatography, samples were dried under a N_2 stream and re-dissolved in ethyl acetate.

2.3. GC–MS analysis and quantification

AA enantiomers were analyzed by gas chromatography-mass spectrometry (GC–MS; Agilent 7890A + 5975B) using a chiral column (Altech Chirasi-L-Val, 50 m length, 0.25 mm internal diameter, 0.16 μm film thickness). 1 μL of sample was injected through a splitless inlet at 200 °C, using helium carrier (0.9 mL/min). Individual amino acids

were separated using a 4-ramp, 57.5 min temperature program: 45 °C start; 2 °C/min to 75 °C; 4 °C/min to 110 °C; 1 °C/min to 125 °C; 4 °C/min to a final temperature of 200 °C. Quantification was based on retention times for authentic D and L standards of each AA, coupled with ion peak areas obtained using single-ion monitoring, based on the following characteristic ion fragments (m/z): Alanine (Ala), 140; valine (Val), 168.1; threonine (Thr), 153; glycine (Gly), 126; isoleucine and leucine (Ile and Leu), 182.1; serine (Ser), 138; proline (Pro), 166.1; aspartic acid/asparagine (Asx), 184; glutamic acid/glutamine (Glx), 180; and phenylalanine (Phe), 190.1. Total amino acid yields, and relative abundance were quantified using mixed L-AA standards in a linear four-point calibration curve ranging from 1 to 1000 μmol/AA. For each AA, peak areas for both enantiomers were converted to molar quantities using a calibration curve for the corresponding ion fragment. Molar percentage abundance (Mol%) for each AA measured was calculated using the sum of the D and L enantiomers.

2.4. Racemization corrections and data analysis

Measured AA enantiomeric ratios were corrected for racemization during sample preparation following the approach of Kaiser and Benner (2005). This approach corrects for racemization during hydrolysis by combining the average racemization for free AAs and the AAs in a protein, measured by Kaiser and Benner (2005). Final racemization corrections consist of two main components: racemization during hydrolysis, and subsequent racemization during derivatization. Since our hydrolysis conditions are identical to those examined in Kaiser and Benner (2005), we used their previously published hydrolysis corrections. However, we also independently quantified the racemization occurring under the analytical conditions used for this study, based on replicate measurements of the average %D-AA in a pure L-AA standard mixture. The racemization-corrected %D-AA we report considers both the hydrolysis and racemization blanks, calculated as described by Kaiser and Benner (2005) (see Appendix section 2.0). Finally, we also tested for potential racemization during our cation-exchange chromatography purification, a step which uses ammonium hydroxide to elute AAs that has not previously been included or tested in a D-AA analysis protocol. Similar to the racemization quantifications experiments discussed above, we used an L-AA standard mixture containing 9 AAs and measured the D/L AA ratio with and without this purification step. There was no observed increase in D-AA abundance beyond our racemization blanks for any of the analyzed AAs introduced by this process (appendix Fig. 1).

Statistical analysis was conducted using the JMP statistical software package (SAS, Version 12). Statistical significance of the difference between means was determined using *t*-tests, with significance levels stated in the text. Relationships between variables are described using orthogonal least-squares regressions, with the ratio of the x and y measurement error variance determined from univariate variance estimates of the x and y variables. Relevant p-values are noted in the text.

3. RESULTS

3.1. Amino acid Mol%

The relative molar abundance of AAs in our two DOM fractions (Fig. 1) is generally comparable to previous measurements in ocean DOM (McCarthy et al., 1998; Kaiser and Benner, 2009). Ala and Gly are the most abundant AAs in both HMW and LMW DOM; averaged across both fractions these AA make up $16 \pm 5\%$ and $22 \pm 5\%$ of the total AAs respectively. Asx and Glx are the next most abundant, with Mol% values of $13 \pm 5\%$ and $8 \pm 2\%$ respectively. The remaining AAs on average each represent $4 \pm 1\%$ of the total AA pool. However, there are also several clear differences in Mol% distributions between LMW and HMW fractions. Ala and Gly have the greatest Mol% offset between DOM size fractions (Fig. 1), however, the two AAs have opposite relationships with respect to MW. The Mol% of Ala is approximately 7% lower in the LMW fraction ($T = 3.45$, $df = 14$, $p < 0.01$), whereas Mol % of Gly is approximately 7% higher ($T = 3.06$, $df = 14$, $p < 0.01$).

In addition to the large Mol% offsets for Ala and Gly between fractions, there are smaller, but significant ($p \leq 0.05$), offsets in Mol% of Asx, Phe, Val, Thr, Ile, and Pro between the size classes. Among these AAs, Asx and Thr are elevated in the HMW fraction, whereas Phe, Val, Ile, and Pro are more abundant in the LMW fraction.

3.2. Amino acid D/L ratios

The D/L ratios of the four D-AAs that have been widely reported in marine HMW DOM literature (Ala, Asx, Ser, and Glx) range from 0.2 to 0.7 (Fig. 2), consistent with previous measurements of similar HMW material (McCarthy et al., 1998; Kaiser and Benner, 2008; Appendix Fig. 2). The D/L ratios in the LMW fraction are generally higher than in the HMW fraction, with the exception of Ala, in which this trend is the opposite. D-Ala also has the largest and most significant offset between HMW and LMW fractions of the 4 previously reported D-AAs (average offset $= 0.21 \pm 0.14$, $T = 4.38$, $df = 14$, $p < 0.01$). The D/L ratio of Ala is also generally the highest of all the chiral AAs (Average D/L $= 0.55 \pm 0.16$). The D/L ratios of all AAs other than Ala are always higher in the LMW fraction relative to HMW (average offset $= 0.11 \pm 0.05$). The general offsets in D/L ratios are consistent at all depths sampled.

In addition to the D-AAs reported previously, we report here for the first time three additional D-AAs. These D-AAs (D-Leu, D-Val, and D-Phe) all have large and significant ($p > 0.01$) offsets in D/L ratios between HMW and LMW fractions (average offset $= 0.12 \pm 0.05$), largely driven by the very low D/L ratios (average D/L $= 0.05 \pm 0.02$) within the HMW fraction (Fig. 2). All three D-AAs were positively identified by GC–MS fragmentation patterns, and the reported abundance and D/L ratios were corrected for both racemization and derivatization blanks, as described previously (see experimental methods 2.4; appendix 2.0). Finally, it should also be noted that despite

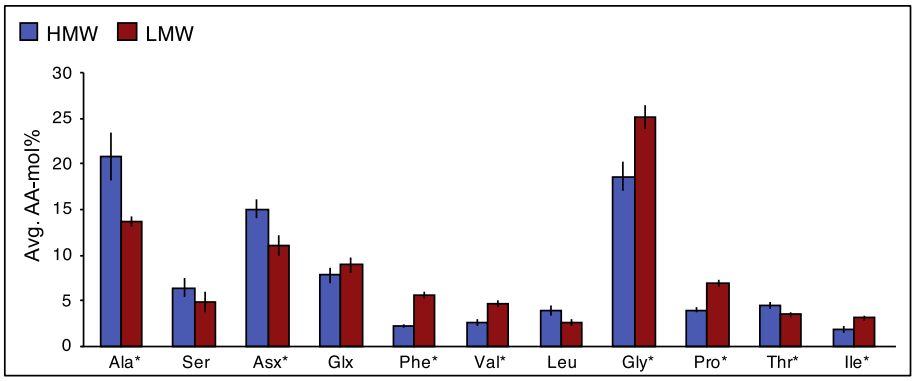

Fig. 1. Average AA Mol% in HMW Semi-Labile and LMW Refractory DOM Fractions. The relative distribution of most AAs is generally similar for both fractions. Ala and Gly are the most abundant AAs in both HMW and LMW DOM; averaged across both fractions these AA make up an average of 16 ± 5% and 22 ± 5% of the total AAs respectively. However, Mol%-Ala is highest in HMW DOM while Mol%-Gly is highest in LMW DOM. In addition, the relative Mol% of Asx and Thr are higher in HMW DOM, whereas Phe, Val, Pro, and Ile have higher relative abundance in LMW DOM. Blue bars = AA-Mol% distribution in HMW UDOM, red bars = AA-Mol% distribution in LMW SPE-DOM. Error bars represent the standard error of the mean AA-Mol% across depth- and cruise-averaged values (n = 8). Stars (*) indicate AAs for which the Mol% offset between fractions is significant (*t*-test, $p \leq 0.05$).

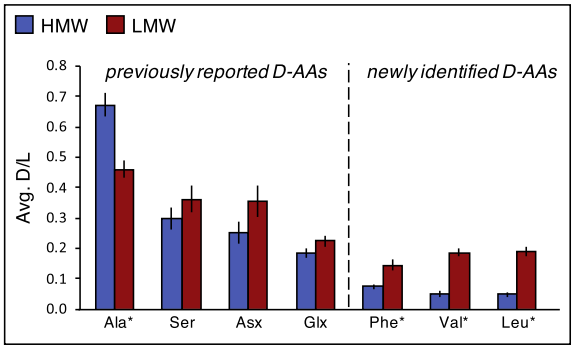

Fig. 2. Average AA D/L ratio in HMW Semi-Labile and LMW Refractory DOM Fractions. The average AA D/L ratio is higher in the LMW refractory DOM fraction compared to HMW semi-labile DOM for all AAs except for Ala. "Previously reported" refers to D-AAs that have been commonly identified in the literature in both HMW and total DOM. "Newly identified" refers to D-AAs confirmed in DOM here for the first time, based on GC–MS fragmentation patterns. Blue bars = D/L ratio in HMW UDOM, red bars = D/L ratio in LMW SPE-DOM. Error bars represent the standard error of the mean D/L ratio across depth- and cruise-averaged values (n = 8). Stars (*) indicate AAs for which the D/L offset between fractions is significant (*t*-test, $p \leq 0.01$). (For interpretation of the references to colour in this figure legend, the reader is referred to the web version of this article.)

the large ^{14}C age offset between the HMW and LMW fractions, the observed offsets in D/L ratio between fractions cannot be due to abiotic racemization alone. For example, in 3500 years (approximately the 14C age offset between HMW and LMW fractions at 2500 m) abiotic racemization of Phe would be expected to increase its %D abundance by 1.4% (Bada, 1971), however the %D-AA of LMW Phe at that depth is approximately 50% higher than in the younger HMW material.

3.3. Water column structure of [D-AA], D/L ratio and AA Mol%

The concentration of individual D-AAs through the water column largely mirrors that of the total DOM pool, with the highest concentrations in the surface, decreasing with depth to a relatively constant value below 850 m, consistent with expectations for a dominant surface derived source (Appendix Fig. 3). The average total D-AA concentration in the surface ocean is 9.4 ± 0.1 nM in the HMW fraction and 3.0 ± 0.2 nM in the LMW fraction. In the deep ocean (2500 m) the total D-AA abundance decreases to 2.4 ± 0.1 nM and 1.2 ± 0.1 nM in the HMW and LMW fractions respectively. Consistent with D/L ratio trends described above, D-Ala is by far the most abundant D-AA, with concentrations as high as 8 nM in surface HMW material. The three newly reported D-AAs (D-Phe, D-Leu, and D-Val) have the lowest concentration throughout the water column, with sub-nM concentrations in both MW fractions. Despite the oceanographic consistency of concentration profiles, there are some variations in the relative proportions of different AAs through the water column, most notably in excursions of the Mol% of Gly, Ala, Phe, and Leu at 400 m (Appendix Fig. 4). There is also notable depth variation in D/L ratio of select AAs, however, only the "new" D-AA (Leu, Val, and Phe) have significant changes in D/L ratio with depth, specifically Leu and Val, which have a clear structure with statistically significant offsets between both surface and subsurface and HMW and LMW fractions (Fig. 3). For these AAs, D/L ratios are lowest in the surface, increasing to maximum values at 400, then decreasing again to apparently constant value in the deep ocean (i.e., similar values observed at 850 m and 2500 m). While these trends are generally consistent for both HMW and LMW fractions, the structure is exaggerated in the LMW fraction, based on a greater elevation of D/L ratio of both Leu and Val at 400 m in the LMW SPE-DOM samples. There is also some depth struc-

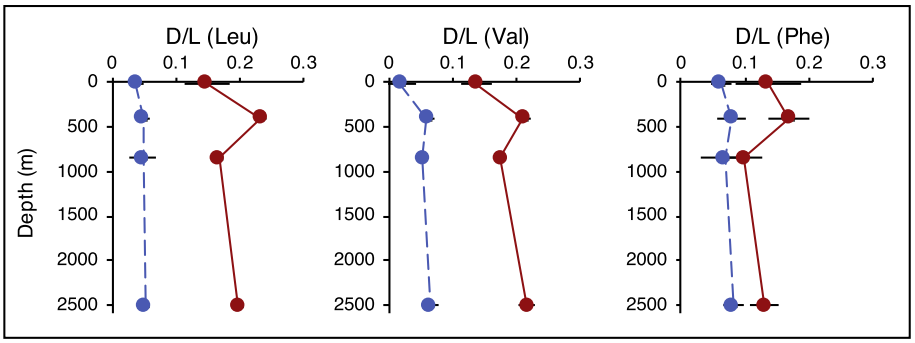

Fig. 3. AA D/L Ratio Depth Profiles in HMW Semi-Labile and LMW Refractory DOM Fractions (Leu, Val, Phe only). All three of the "newly identified" D-AAs (Leu, Val, and Phe) have significant changes in D/L ratio with depth within the LMW fraction, specifically Leu and Val, which have a clear structure with statistically significant offsets between surface and subsurface and maxima at 400 m. Each point represents the average value of duplicate sampling seasons. Blue symbols, dashed line = HMW DOM; red symbols, solid line = LMW SPE-DOM. Error bars represent the propagated standard error associated with racemization corrections and season-averaged D/L ratios. (For interpretation of the references to colour in this figure legend, the reader is referred to the web version of this article.)

ture in the D/L ratio of Phe (Fig. 3), however only in the more refractory LMW fraction, with a maximum Phe D/L ratio at 400 m decreasing to consistently lower values below 850 m, but no significant offset between the surface and 400 m. The lack of any significant depth structure in D/L ratio among the other D-AAs (Appendix Fig. 3) is consistent with previous published D/L measurements of Ala, Asx, Glx, and Ser in both HMW and total DOM (McCarthy et al., 1998; Nagata et al., 2003; Pèrez et al., 2003; Kaiser and Benner, 2008; Kaiser and Benner, 2009).

3.4. Relationships between D/L ratio, Mol% AA, and $\Delta^{14}C$

The D/L ratio and Mol% of individual AAs are directly linked across the entire size/age spectrum of marine DOM (Fig. 4). At the individual AA level, AAs with higher Mol% have greater contributions of their D-enantiomer, regardless of season, depth, or size class. This correlation is individually stronger within the HMW fraction ($R^2 = 0.86$) than in the LMW fraction ($R^2 = 0.69$) (Appendix Fig. 4), largely driven by the very high abundance and D/L ratio of Ala within the HMW fraction. However, even with Ala removed, a significant correlation between Mol% and D/L ratio remains for all other AA ($R^2 = 0.47$; Appendix Fig. 5).

In contrast to Mol%, there was generally little linear correlation between D/L ratio of individual AAs and $\Delta^{14}C$ age of corresponding HMW or LMW DOM samples. However, there were clear offsets in AA D/L ratios between old and young material, corresponding to the ^{14}C ages in LMW and HMW DOM fractions respectively. When all samples are considered together, there are apparent significant correlations ($p < 0.05$) between the D/L ratio and $\Delta^{14}C$ for three AAs: Phe, Val, and Leu (Fig. 5; left panel). However, when considered within either HMW or LMW fractions individually these correlations are no longer statistically significant (Fig. 5; right panel), suggesting that change in D/L ratio of these AAs may not actually be linearly related throughout the entire age/size spectrum. Ala also had substantial offsets between D/L ratios in older LMW material and younger HMW material, however no statistically significant correlations within MW fractions (Figs. 5 and 6). As noted above, D-Ala was also unique in that the D/L ratios were offset in the opposite direction compared to all the other D-AAs (i.e., more D-enantiomer in the younger, HMW material) (Fig. 6). Finally, for three AAs (Asx, Ser, and Glx) there were no correlations with DOM age, and no offsets between MW fractions (Appendix Fig. 6). Overall, for all D-AAs except for these three, there appears to be clear offsets in D/L ratio at all depths between the two MW fractions, however little evidence for a continuous relationship between DOM age and D/L ratio.

4. DISCUSSION

Prokaryotic organisms dominate the synthesis and incorporation of D-AAs in the marine environment. D-AAs are a ubiquitous component of bacterial biomolecules such as in the peptide inter-bridge of bacterial peptidoglycan, providing one of the few unambiguous molecular tracers for bacterially synthesized AAs. As such, D-AAs are one of the most widely used tracers for bacterial influence in biogeochemical cycles and have been used as indicators of the contribution of bacterial carbon or nitrogen in a number of environments such as marine and lacustrine DOM and sediments (McCarthy et al., 1998; Grutters et al., 2002; Benner and Kaiser, 2003; Jorgensen et al., 2008; Carstens and Schubert, 2012; Carstens et al., 2012). Further, because D-AAs are contained within a major biochemical constituent of the DON pool, they can provide a more direct tracer for microbial contributions to the DON pool than extrapolations from DOC properties. Therefore, the significant ^{14}C age differences between our HMW and LMW DOM fractions combined with the elevation of D/L ratio across all D-AAs (except Ala) within the LMW fraction suggests that there is a larger prokaryotic contribution to LMW refractory marine DOM than the fresher HMW DON pool.

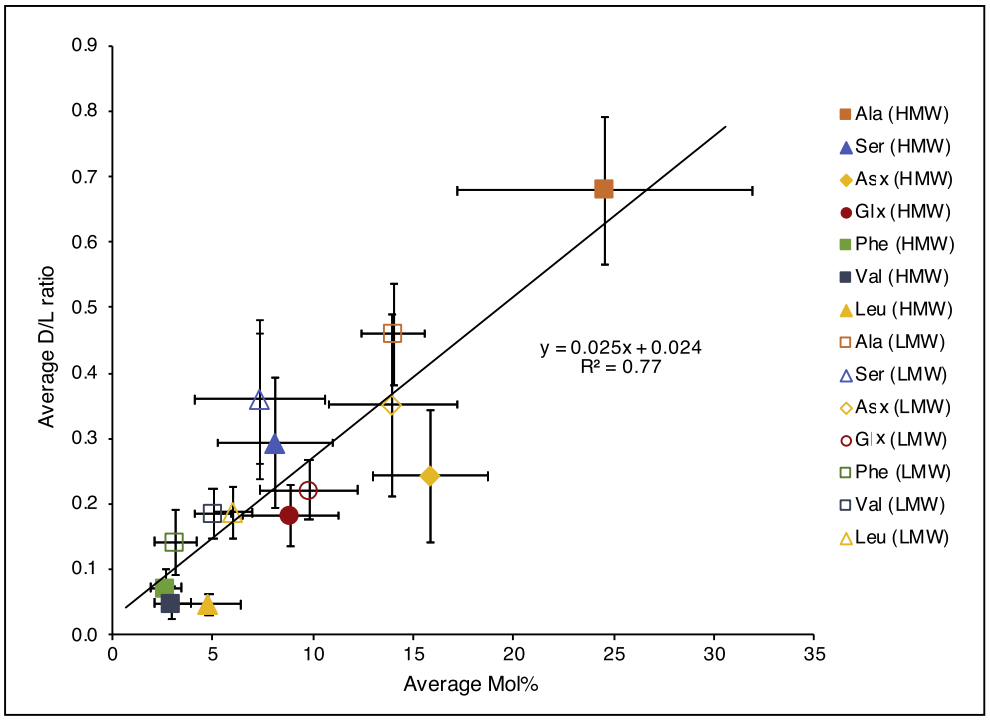

Fig. 4. Positive Correlation Between AA-Mol% and D/L Ratio Across All Amino Acids in Both HMW Semi-Labile and LMW Refractory DOM Fractions. Each point represents the average Mol% and D/L ratio of all samples for each AA, error bars represent the standard deviation of all samples (n = 8). $R^2 = 0.77$, t = 6.4, df = 14, $p > 0.01$.

4.1. D-AA comparison to previous measurements of HMW UDON and total LMW DON

The measured D/L ratios for the four D-AAs that have been widely reported in DOM (Ala, Asx, Ser, and Glx) correspond closely with previous direct measurements in HMW UDOM, and also with D/L ratios for LMW DOM previously calculated by difference (e.g., McCarthy et al., 1998, Kaiser and Benner, 2008; Appendix Fig. 2). The similar D/L ratios in the HMW DOM pool are not unexpected, however this comparison confirms that the specific protocol used here, including the new cation-exchange purification and our derivative-specific racemization corrections, yield results directly comparable with past approaches.

The similarity for the D/L ratios measured directly in our LMW SPE-DOM fraction and those previously calculated for total LMW DOM are more noteworthy. The prior LMW results (Kaiser and Benner, 2008) were derived by difference (total DON minus HMW UDON) for the entire operational LMW pool (~75–90% of total DON permeating a UF membrane). The fact that these values are identical within error to our direct measurements is remarkable, given the completely different sampling times, isolation, and subsequent analysis conditions. Most important, this result suggests that our new coupled UF/SPE isolation protocol, despite directly recovering only 20–40% of LMW DOM, captures a representative fraction of the LMW AA pool. This conclusion is further supported by available $\delta^{15}N$ data, which suggests the portion of LMW DON we capture is also isotopically representative of the total LMW pool's $\delta^{15}N$ values (Broek et al., 2017). Together, this highlights a major advantage of our new method: because of the low concentration of D-AAs in deep ocean DOM, calculations that rely on mass balance to determine the properties of the LMW DOM pool are associated with high uncertainty. In contrast, direct measurements on large, organic–rich isolates can be far more precise, allowing a wider variety of direct molecular measurements compared to quantification at ambient concentrations.

4.2. Unique behavior of D-Ala: a potential tracer for peptidoglycan and labile HMW bacterial material

Ala emerged as unique across multiple aspects of our data set. D-Ala is the most abundant D-AA in all samples, and the relationship between the D/L ratio of Ala and DOM age and molecular weight is consistently the opposite from that of all other D-AAs (Fig. 2). These observations are also consistent with trends in Mol% (Fig. 1), together suggesting that D-Ala may be uniquely associated with highly labile bacterial source biochemicals with more rapid cycling than other D-AA containing compounds. This observation is also consistent with a maximum in Mol% Ala at 400 m in the HMW fraction (Appendix Fig. 4), suggesting that microbial processes in the water column contribute Ala predominantly to the HMW DOM pool. Multiple studies examining relative AA abundance changes with degradation have found that Mol% Ala generally increases with microbial alteration (Dauwe et al., 1999;

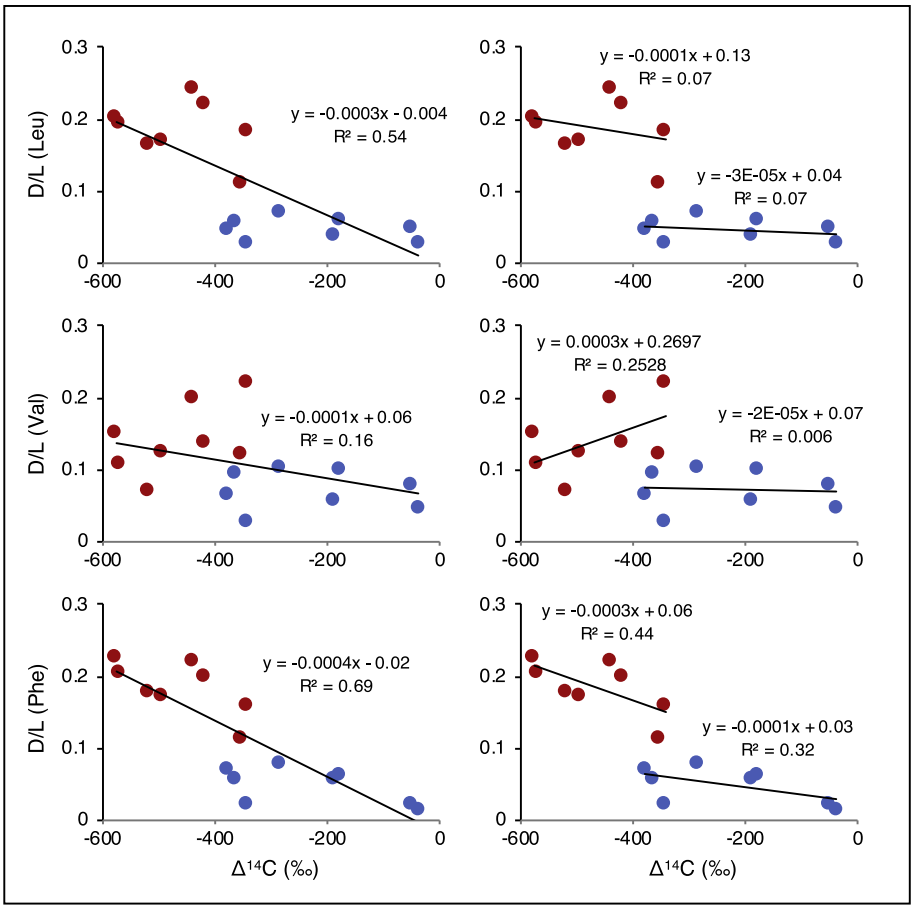

Fig. 5. D/L Ratio vs. $\Delta^{14}C$ of AAs with Significant D/L Offsets Between HMW Semi-Labile and LMW Refractory DOM Fractions (Leu, Val, Phe). The three "newly identified" D-AAs (Leu, Val, and Phe) have significant offsets in average D/L ratio between HMW semi-labile and LMW refractory DOM fractions. As a result, when all samples are considered together, there are significant correlations ($p < 0.05$) between the D/L ratio and $\Delta^{14}C$ (left panel). However, when considered within either HMW or LMW fractions these correlations are no longer statistically significant (right panel), suggesting that change in D/L ratio of these AAs may not actually be linearly related throughout the entire age/size spectrum. Each point represents a single sample. Red symbols = LMW SPE-DOM, blue symbols = HMW UDOM. (For interpretation of the references to colour in this figure legend, the reader is referred to the web version of this article.)

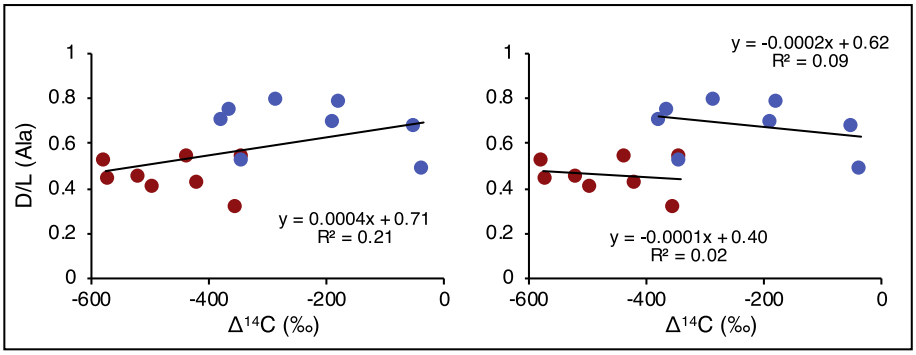

Fig. 6. D/L ratio vs. $\Delta^{14}C$ of Alanine. Similar to Leu, Val, and Phe, the average D/L ratio of Ala is significantly different between HMW semi-labile and LMW refractory DOM fractions. As a result, when all samples are considered together, there are significant correlations ($p < 0.05$) between the D/L ratio and $\Delta^{14}C$ (left panel). However, when considered within either HMW or LMW fractions these correlations are no longer statistically significant (right panel), suggesting that change in D/L ratio of these AAs may not actually be linearly related throughout the entire age/size spectrum. Each point represents a single sample. Red symbols = LMW SPE-DOM, blue symbols = HMW UDOM. (For interpretation of the references to colour in this figure legend, the reader is referred to the web version of this article.)

Lee et al., 2000; Yamashita and Tanoue, 2003; Calleja et al., 2013). Within this framework, coupled with size-reactivity relationships, our results are unexpected. Past observations would predict that LMW DOM should be more degraded, and so might be expected to have both more total Ala and higher D/L Ala ratios. However, in our data, the higher D/L ratio and Mol% values in HMW DON compared to LMW DON suggests that biomolecules most enriched in D-Ala are concentrated in the HMW pool, and that D-Ala progressively grows into only the HMW pool with microbial processing.

We hypothesize that the most likely D-Ala source consistent with these observations is peptidoglycan, a structural polymer containing D-AAs, which is a major component of bacterial cell walls (Schleifer, 1972; McCarthy et al., 1998). Peptidoglycan is a large polymerized macromolecule, which has been shown to be quite labile in seawater, with particularly rapid remineralization of the peptide component after hydrolysis (Nagata et al., 2003). Based on carbohydrate to D-AA ratios, previous work has indicated that intact peptidoglycan subunits likely constitute <0.1% of DON (Kaiser and Benner, 2008). While this might rule out the hypothesis of a main peptidoglycan source, there is evidence that degradation of peptidoglycan may obscure estimates based on molecularly identifiable sugar monomers. The work of Nagata and coauthors used radiolabeling experiments to show that intact peptidoglycan is rapidly broken into smaller molecular fragments during microbial degradation which are both resistant to further degradation, and importantly are no longer identifiable by standard chromatographic techniques (Kitayama et al., 2007). These direct marine degradation experiments suggest that peptidoglycan added to the dissolved phase would likely be rapidly degraded and structurally modified, such that intact D-Ala originally contained in peptide interbridges would not persist within the refractory LMW pool. It should also be noted that despite the dominance of D-Ala as a major component of peptidoglycan in cell walls, D-Ala also has other possible bacterial molecular sources such as lipopolysaccharides and lipopeptides (Kaiser and Benner, 2008). We therefore cannot exclude the possibility that other relatively labile, D-Ala rich microbial biomolecules could also contribute to these trends.

4.3. "New" D-AAs: potential tracers for refractory DON production

A novel aspect of our data is the identification of three D-AAs (D-Phe, D-Leu, and D-Val) not previously identified in the DOM literature, but present in all of the samples measured for this study. While some prior work has suggested the presence of minor amounts of these compounds in HMW DOM (McCarthy et al., 1998; Yamaguchi and McCarthy, 2018), reported abundances were both low and inconsistent, often indistinguishable from blanks. This is likely explained by the much lower abundance of these compounds in HMW UDOM samples compared to our LMW fraction. Further, earlier GC-FID or LCMS data was not able to make positive molecular identifications; DOM hydrolysate mixtures are notoriously complex, with multiple small and often overlapping peaks that cannot readily be identified based only on retention times (McCarthy and Bronk, 2008; Yamaguchi and McCarthy, 2018). In our data, GC–MS fragmentation data and quantification based on single-ion monitoring unambiguously shows that in addition to the four D-AAs widely measured in DOM previously, these three D-AAs are present in every DOM sample. Finally, the measurements of LMW DON D/L ratios of these D-AAs would likely not be possible with current instrumentation without the direct isolation and concentration of LMW DON used in our protocols.

The observations of strong enrichment of these D-AAs in LMW DOM relative to HMW DOM (Fig. 2), as well as the clear depth trends in the LMW fraction (including observed maxima at 400 m; Fig. 3), suggest these novel D-AAs are most strongly linked to the production of LMW, refractory DOM. While all D-AAs measured (except for D-Ala, as discussed above) were more abundant in older, LMW material, the relationships for D-Val, D-Leu, and D-Phe are clearly distinct. Of all 7 D-AAs we measured in this study, only these had clear and repeatable structure in D/L ratio with depth between cruises. The synchronous depth structure for these compounds (Fig. 3) supports the hypothesis that they trace the same source material, with cycling in the upper water column distinct from the other D-AAs. More significantly, however, the variable behavior of AAs at 400 m compared to the other depths suggests that local processes are resulting in active transformations within or additions to the LMW pool. This depth is within the "twilight zone" region of maximum particle flux attenuation, where sinking material from the euphotic zone is most rapidly remineralized by heterotrophic bacteria (Buesseler et al., 2007). While we do not have enough resolution to assess if 400 m in fact represents the exact maxima or minima in our measurements, we hypothesize that the offsets from surface to 400 m could be influenced by input of fresh, heterotrophic bacterial material. This demonstrates that despite the old average age of LMW DON, at least a portion of this material in the mesopelagic is involved in active cycling processes operating on timescales much shorter than that of ocean circulation. We also note that the waters around 400 m at Station Aloha are ventilated in the North Pacific outside of the subtropical gyre. Therefore, it is possible that the waters at this depth bear some unique signature of this other water mass. However, we have not observed any clear evidence for the influence of this water mass in other properties of our isolated DOM fractions (such as an inversion in ^{14}C age). Further, significant offsets in our measured properties between adjacent water masses would still be consistent with transformations of both the HMW and LMW fractions occurring on time scales much less than that of global ocean circulation.

To our knowledge, there are no currently known marine bacterial sources of D-Leu, D-Val, and D-Phe. While future work will therefore be required to identify the molecular sources of these compounds, these observations suggest they trace the same, or perhaps very similar, classes of bac-

terial biomolecules. We hypothesize that these compounds may be useful new tracers for understanding microbial production of the most refractory DOM.

Finally, we note that Gly, despite being a major AA in HMW DOM (and dominating AA Mol% in LMW DOM), cannot be included in a similar analysis since Gly is non-chiral, and so has no D-enantiomer. However, its elevated Mol% within the LMW SPE-DOM fraction suggests that it might also be a useful AA for tracking the production of refractory LMW DON. This is consistent with the studies discussed in Section 4.2 which demonstrated that Ala and Gly represent the most useful AAs for tracking microbial influence in total organic matter (Dauwe et al., 1999; Lee et al., 2000; Yamashita and Tanoue, 2003; Kaiser and Benner, 2012; Calleja et al., 2013). We hypothesize that measuring the $\delta^{15}N$ value of Gly might be one way to directly test this idea, since $\delta^{15}N_{Gly}$ has been shown to increase dramatically (+10 to +15‰ increase) during bacterial degradation of DOM (Calleja et al., 2013).

4.4. DOM ^{14}C age, MW fractions and D/L ratios: implications for a microbial N pump & DON size-reactivity "continuum"

This data set has allowed us to directly test the microbial N pump idea and investigate the hypothesis that microbes are directly responsible for the production of refractory DON and the associated sequestration of N within the marine DON pool. We hypothesized that a continuous relationship between AA-D/L ratio and DOC $\Delta^{14}C$ would indicate a progressive increase in microbial influence along a size-reactivity continuum, with slopes reflecting relative rates of input for individual D-AA sources. In contrast, size-based discontinuities in slopes might indicate distinct sources for different D-AAs or unique degradation processes within the semi-labile and refractory DOM pools.

Our primary finding of higher overall D/L ratios in older, LMW material relative to younger HMW DOM strongly supports our basic hypothesis. However, the unexpected finding that there are little to no significant trends between D/L ratios and $\Delta^{14}C$ which apply across both MW fractions was in contrast to our original hypothesis. The apparent discontinuity between HMW and LMW in the $\Delta^{14}C$ regressions suggests that the behavior of these D-AAs might be more consistent with separate sources to HMW and LMW DON. This interpretation is an apparent departure from a size-reactivity "continuum" prediction, where LMW is derived from the degradation of HMW material. It would instead suggest a somewhat more complicated relationship, with more independent HMW and LMW DON pools, perhaps formed from different surface sources, or through different mechanisms. As mentioned above, the D-AA depth trends within the LMW material suggest it is being transformed on timescales much shorter than global ocean circulation, and the unique behavior of different AAs in each MW fraction demonstrates active cycling in both fractions. At the same time, the variation in distribution and apparent behavior of both fractions supports the idea that D-AAs likely have distinct microbial source biomolecules, as suggested by Kaiser and Benner (2008), as well as likely diversity in the cycling dynamics of the sources traced by each group.

The unified relationship between D/L ratio and molar abundance across all D-AAs (Fig. 4) was also an unexpected finding. Because of the greater number of D-AAs measured here, including the newly confirmed D-AAs that exist at low concentrations in both size classes, this relationship likely could not have been identified in past work. Overall, this apparent coupling of D/L ratio and molar abundance links bacterial source with relative AA concentration across all seven chiral AAs we now recognize in marine DOM, indicating that the most abundant AAs derive disproportionately from non-protein bacterial sources. This suggests that the relative abundance of all AAs within marine DOM is predominantly shaped by input from prokaryotic sources.

5. SUMMARY AND CONCLUSIONS

To test the "microbial N pump" hypothesis, we measured AA enantiomers and AA Mol% distributions in conjunction with ^{14}C ages for independently isolated HMW and LMW DOM fractions. D-AAs are direct biomarkers for prokaryotic source within the largest identifiable DON compound class and $\Delta^{14}C$ data provides an average age for each DOM fraction as a proxy for reactivity. Coupling these measurements allowed a first direct assessment of the prokaryotic contribution to different DON pools with greatly contrasting ages, recalcitrance, and bulk chemical properties, from the surface to the deep ocean in the North Pacific Subtropical Gyre.

When Ala is excluded, total D-AA abundances are highest in the samples with the oldest ^{14}C age, strongly supporting the idea that prokaryotic organisms represent a direct source of refractory DON. We observed similar D/L ratios as previously published work for the four AAs widely reported in marine DOM (Ala, Asx, Glx, and Ser) in both HMW and LMW material. However, GC–MS analysis also allowed identification and quantification of three additional D-AAs (D-Leu, D-Val, and D-Phe) present at all depths in all samples, although strongly concentrated in LMW DOM. Despite the lower concentrations of these newly confirmed D-AAs, their concentration profiles show oceanographically consistent trends within and between size fractions, confirming that they are real compounds with unique tracer potential. We observed consistent and unique relationships between D/L ratio, AA-Mol%, and $\Delta^{14}C$ among different AAs, suggesting that a number of key D-AA subgroupings may represent unique proxies for specific bacterial sources.

D-Ala emerged as unique within almost all aspects of our data set. Consistent with previous reports, D-Ala was the single most abundant D-AA in our DOM samples. However, in contrast to the relationship between D/L ratio and ^{14}C age for all the other D-AAs, we observed lower D/L ratios of Ala in the older, refractory, LMW DOM fraction, and higher D/L ratios in the younger, semi-labile, HMW fraction. This distinct relationship was accompanied by analogous Mol% trends, with significantly lower Mol% Ala in refractory DOM compared with semi-labile DOM.

We therefore hypothesize that D-Ala cycling is linked to the input and subsequent degradation of semi-labile peptidoglycan material. This is in contrast to other D-AAs, which may have more diverse bacterial origins and slower degradation rates.

Aside from Ala, the offset in D/L ratios between semi-labile HMW and refractory LMW DOM was largest for the newly confirmed D-AAs, suggesting these may be the best D-AA tracers for bacterial contribution to the refractory DON pool. Further, the depth trends in both AA Mol% and D/L ratio are nearly identical for these AAs, suggesting that they may trace the same microbial source materials. The minimum and maximum of AA Mol% and D/L ratio respectively in the upper mesopelagic also suggest a potential linkage to sinking particle sources. Future work will be required to investigate the most likely biomolecular sources for these D-AAs, however we hypothesize that together D-Val, D-Leu, and D-Phe have potential as new tracers for the most refractory bacterial material accumulating in the ocean's DON pool. Overall, our data suggests that within the expanded group of 7 D-AAs now identified, subgroups of D-AAs trace individual microbial sources with unique cycling rates and demonstrates a significant expansion of tracer potential for D-AAs in ocean DOM.

Together, our data set strongly supports a microbial N pump, however, not necessarily one that operates exactly as expected from the current interpretation of a DOM size-age "continuum". While the D-AA enantiomers are generally concentrated within the refractory LMW pool, the lack of continuity in D/L ratio across a ^{14}C age spectrum raises the possibility that although refractory LMW DON has a clear microbial source, it is not necessarily derived from microbial degradation of semi-labile HMW DON, but rather from independent microbial sources in the upper ocean. We caution, however, that this interpretation is in part based on the assumption that trends in DON or AA ^{14}C ages generally follow those of total DOM, and also that they are mostly surface derived. While this seems very likely based on past work (Loh et al., 2004) as well as methodological tests with both ultrafiltration (Walker et al., 2011) and SPE sorbents (Flerus et al., 2012; Broek et al., 2017), we suggest that future work aimed at both determining exact ages of purified AAs in the ocean, coupled with an expanded understanding of specific molecular sources of different D-AAs, could lead to a far more detailed mechanistic understanding of how different bacterial communities contribute to the formation of refractory DON in the oceans.

ACKNOWLEDGMENTS

The authors would like to thank Elizabeth Gier and Hilary Close for assistance with GC-MS instrumentation, analytical protocols, and interpretation of amino acid D/L and Mol% data. This work was supported by a grant from NSF Chemical Oceanography (Award # 1358041).

APPENDIX A. SUPPLEMENTARY MATERIAL

Supplementary data to this article can be found online at https://doi.org/10.1016/j.gca.2018.12.037.

REFERENCES

Alkhatib M., Schubert C. J., del Giorgio P. A., Gelinas Y. and Lehmann M. F. (2012) Organic matter reactivity indicators in sediments of the St. Lawrence Estuary. *Estuar. Coast. Shelf Sci.* **102–103**, 36–47.

Aluwihare L. I., Repeta D. J. and Pantoja S. (2005) Two chemically distinct pools of organic nitrogen accumulate in the ocean. *Science* **308**, 1007–1010.

Arrieta J. M., Mayol E., Hansman R. L., Herndl G. J., Dittmar T. and Duarte C. M. (2015) Dilution limits dissolved organic carbon utilization in the deep ocean. *Science* **348**, 331–333.

Bada J. L. (1971) Kinetics of the nonbiological decomposition and racemization of amino acids in natural waters. Am. Chem. Soc. *Adv. Chem. Ser.* **106**, 309–331.

Benner R. and Amon R. M. W. (2015) The size-reactivity continuum of major bioelements in the ocean. *Annu. Rev. Marine. Sci.* **7**, 185–205.

Benner R. and Kaiser K. (2003) Abundance of amino sugars and peptidoglycan in marine particulate and dissolved organic matter. *Limnol. Oceangr.* **48**, 118–128.

Benner R. and Ziegler S. (1999) Do photochemical transformations of dissolved organic matter produce biorefractory as well as bioreactive substrates. In Microbial Biosystems: New Frontiers. Proceedings of the 8th International Symposium on Microbial Ecology (eds. C. R. Bell, M. Brylinsky, P. Johnson-Green). Atlantic Canada Society for Microbial Ecology, Halifax. pp. 181–192.

Broek T. A. B., Walker B. D., Guilderson T. P. and McCarthy M. D. (2017) Coupled ultrafiltration and solid phase extraction approach for the targeted study of semi-labile high molecular weight and refractory low molecular weight dissolved organic matter. *Mar. Chem.*, 1–36.

Bronk D. A., See J. H., Bradley P. and Killberg L. (2007) DON as a source of bioavailable nitrogen for phytoplankton. *Biogeosciences* **4**, 283–296.

Buesseler K. O., Lamborg C. H., Boyd P. W., Lam P. J., Trull T. W., Bidigare R. R., Bishop J. K. B., Casciotti K. L., Dehairs F., Elskens M., Honda M., Karl D. M., Siegel D. A., Silver M. W., Steinberg D. K., Valdes J., Van Mooy B. and Wilson S. (2007) Revisiting carbon flux through the Ocean's twilight zone. *Science* **316**, 567–570.

Calleja M. L., Peacock M., Kudela R. and Batista F. C. (2013) Changes in compound specific δ 15 N amino acid signatures and d/l ratios in marine dissolved organic matter induced by heterotrophic bacterial reworking. *Mar. Chem.* **149**, 32–44.

Carstens D. and Schubert C. J. (2012) Amino acid and amino sugar transformation during sedimentation in lacustrine systems. *Org. Geochem.* **50**, 26–35.

Carstens D., Köllner K. E., Bürgmann H., Wehrli B. and Schubert C. J. (2012) Contribution of bacterial cells to lacustrine organic matter based on amino sugars and d-amino acids. *Geochim. Cosmochim. Ac.* **89**, 159–172.

Cowie G. L. and Hedges J. I. (1992) Sources and reactivities of amino acids in a coastal marine environment. *Limnol. Oceangr.* **37**, 703–724.

Dauwe B., Middelburg J. J., Herman P. M. J. and Heip C. H. R. (1999) Linking diagenetic alteration of amino acids and bulk organic matter reactivity. *Limnol. Oceangr.* **44**, 1809–1814.

Décima M., Landry M. R. and Popp B. N. (2013) Environmental perturbation effects on baseline δ15N values and zooplankton trophic flexibility in the southern California Current Ecosystem. *Limnol. Oceangr.* **58**, 624–634.

Décima M., Landry M. R., Bradley C. J. and Fogel M. L. (2017) Alanine δ 15N trophic fractionation in heterotrophic protists. *Limnol. Oceangr.* **62**, 2308–2322.

Dittmar T. (2014) Reasons behind the long-term stability of dissolved organic matter. In *Biogeochemistry of Marine Dissolved Organic Matter*. Academic Press, pp. 369–388.

Eglinton T. I. and Repeta D. J. (2006) Organic matter in the contemporary ocean. In *Treatise on Geochemistry, Volume 6: The Oceans and Marine Geochemistry* (ed. H. Elderfield). Elsevier, Amsterdam, pp. 145–180.

Flerus R., Lechtenfeld O. J., Koch B. P., McCallister S. L., Schmitt-Kopplin P., Benner R., Kaiser K. and Kattner G. (2012) A molecular perspective on the ageing of marine dissolved organic matter. *Biogeosciences* **9**, 1935–1955.

Grutters M., van Raaphorst W., Epping E., Helder W., de Leeuw J. W., Glavin D. P. and Bada J. (2002) Preservation of amino acids from in situ-produced bacterial cell wall peptidoglycans in northeastern Atlantic continental margin sediments. *Limnol. Oceangr.* **47**, 1521–1524.

Gweon L. B. and Fisher N. S. (1992) Degradation and elemental release rates from phytoplankton debris and their geochemical implications. *Limnol. Oceangr.* **37**, 1345–1360.

Hansell D. A., Carlson C. A., Repeta D. J. and Schlitzer R. (2009) Dissolved organic matter in the ocean: a controversy stimulates new insights. *Oceanography* **22**, 202–211.

Hedges J. I. (1992) Global biogeochemical cycles: progress and problems. *Mar. Chem.* **39**, 67–93.

Hedges J. I., Eglinton G., Hatcher P. G., Kirchman D. L., Arnosti C., Derenne S., Evershed R. P., Kögel-Knabner I., de Leeuw J. W., Littke R., Michaelis W. and Rullkötter J. (2000) The molecularly-uncharacterized component of nonliving organic matter in natural environments. *Org. Geochem.* **31**, 945–958.

Hertkorn N., Harir M., Koch B. P., Michalke B. and Schmitt-Kopplin P. (2013) High-field NMR spectroscopy and FTICR mass spectrometry: powerful discovery tools for the molecular level characterization of marine dissolved organic matter. *Biogeosciences* **10**, 1583–1624.

Jiao N., Herndl G. J., Hansell D. A., Benner R., Kattner G., Wilhelm S. W., Kirchman D. L., Weinbauer M. G., Luo T., Chen F. and Azam F. (2010) Microbial production of recalcitrant dissolved organic matter: long-term carbon storage in the global ocean. *Nature Publishing Group* **8**, 593–599.

Jorgensen N. O. G., Engel P., Jellison R. and Hollibaugh J. T. (2008) Contribution of bacterial cell wall components to DOM in alkaline, hypersaline Mono Lake, California. *Geomicrobiol. J.* **25**, 38–55.

Jørgensen L., Lechtenfeld O. J., Benner R., Middelboe M. and Stedmon C. A. (2014) Production and transformation of dissolved neutral sugars and amino acids by bacteria in seawater. *Biogeosciences* **11**, 5349–5363.

Schleifer K. H. (1972) Peptidoglycan types of bacterial cell walls and their taxonomic implications. *Bacteriol. Rev.* **36**, 407.

Kaiser K. and Benner R. (2012) Organic matter transformations in the upper mesopelagic zone of the North Pacific: chemical composition and linkages of microbial community structure. *J. Geophys. Res.* **117**, C01023.

Kaiser K. and Benner R. (2009) Biochemical composition and size distribution of organic matter at the Pacific and Atlantic time-series stations. *Mar. Chem.* **113**, 63–77.

Kaiser K. and Benner R. (2008) Major bacterial contribution to the ocean reservoir of detrital organic carbon and nitrogen. *Limnol. Oceangr.* **53**, 99–112.

Kaiser K. and Benner R. (2005) Hydrolysis-induced racemization of amino acids. *Limnol. Oceanogr. – Meth.* **3**, 318–325.

Kirchman D. L. (2004) A primer on dissolved organic material and heterotrophic prokaryotes in the oceans. In The Ocean Carbon Cycle and Climate Springer, Dordrecht, Dordrecht. pp. 31–63.

Kitayama K., Hama T. and Yanagi K. (2007) Bioreactivity of peptidoglycan in seawater. *Aquat. Microb. Ecol.* **46**, 85–93.

Koch B. P., Witt M., Engbrodt R., Dittmar T. and Kattner G. (2005) Molecular formulae of marine and terrigenous dissolved organic matter detected by electrospray ionization Fourier transform ion cyclotron resonance mass spectrometry. *Geochim. Cosmochim. Ac.* **69**, 3299–3308.

Lechtenfeld O. J., Hertkorn N., Shen Y., Witt M. and Benner R. (2015) Marine sequestration of carbon in bacterial metabolites. *Nat. Commun.* **6**, 6711.

Lechtenfeld O. J., Kattner G. and Flerus R. (2014) Molecular transformation and degradation of refractory dissolved organic matter in the Atlantic and Southern Ocean. *Geochim. Cosmochim. Ac.* **126**, 321–337.

Lee C., Wakeham S. G. and Hedges J. I. (2000) Composition and flux of particulate amino acids and chloropigments in equatorial Pacific seawater and sediments. *Deep-Sea Res. PI* **47**, 1535–1568.

Lehmann M. F., Bernasconi S. M., Barbieri A. and McKenzie J. A. (2002) Preservation of organic matter and alteration of its carbon and nitrogen isotope composition during simulated and in situ early sedimentary diagenesis. *Geochim. Cosmochim. Ac.* **66**, 3573–3584.

Loh A. N., Bauer J. E. and Druffel E. R. M. (2004) Variable ageing and storage of dissolved organic components in the open ocean. *Nature* **430**, 877–881.

Mao J., Kong X., Schmidt-Rohr K., Pignatello J. J. and Perdue E. M. (2012) Advanced solid-state NMR characterization of marine dissolved organic matter isolated using the coupled reverse osmosis/electrodialysis method. *Environ. Sci. Technol.* **46**, 5806–5814.

McCarthy M. D. and Bronk D. A. (2008) Analytical methods for the study of Nitrogen. In *Nitrogen in The Marine Environment*. Elsevier, pp. 1219–1275.

McCarthy M. D., Beaupré S. R., Walker B. D., Voparil I., Guilderson T. P. and Druffel E. R. M. (2010). *Chemosynthetic Origin Nat. Geosci.* **3**, 1–5.

McCarthy M. D., Benner R., Lee C. and Fogel M. L. (2007) Amino acid nitrogen isotopic fractionation patterns as indicators of heterotrophy in plankton, particulate, and dissolved organic matter. *Geochim. Cosmochim. Ac.* **71**, 4727–4744.

McCarthy M. D., Benner R., Lee C., Hedges J. I. and Fogel M. L. (2004) Amino acid carbon isotopic fractionation patterns in oceanic dissolved organic matter: an unaltered photoautotrophic source for dissolved organic nitrogen in the ocean? *Mar. Chem.* **92**, 123–134.

McCarthy M. D., Hedges J. I. and Benner R. (1998) Major bacterial contribution to marine dissolved organic nitrogen. *Science* **281**, 231–234.

McCarthy M. D., Pratum T., Hedges J. I. and Benner R. (1997) Chemical composition of dissolved organic nitrogen in the ocean. *Nature* **390**, 150–154.

Moore C. M., Mills M. M., Arrigo K. R., Berman-Frank I., Bopp L., Boyd P. W., Galbraith E. D., Geider R. J., Guieu C., Jaccard S. L., Jickells T. D., La Roche J., Lenton T. M., Mahowald N. M., Marañón E., Marinov I., Moore J. K., Nakatsuka T., Oschlies A., Saito M. A., Thingstad T. F., Tsuda A. and Ulloa O. (2013) Processes and patterns of oceanic nutrient limitation. *Nat. Geosci.* **6**, 701–710.

Nagata T. and Kirchman D. L. (1999) Bacterial mortality: a pathway for the formation of refractory DOM. In *Microbial Biosystems: New Frontiers. Proceedings of the 8th International Symposium on Microbial Ecology* (eds. C. R. Bell, M. Brylinsky and P. Johnson-Green). Atlantic Canada Society for Microbial Ecology, Halifax, pp. 153–158.

Nagata T., Meon B. and Kirchman L. D. (2003) Microbial degradation of peptidoglycan in seawater. *Limnol. Oceangr.* **48**, 745–754.

Niggemann J., Lomstein B. A. and Schubert C. J. (2018) Diagenesis of amino compounds in water column and sediment of Lake Baikal. *Org. Geochem.* **115**, 67–77.

Ogawa H. (2001) Production of refractory dissolved organic matter by bacteria. *Science* **292**, 917–920.

Pèrez M. T., Pausz C. and Herndl G. J. (2003) Major shift in bacterioplankton utilization of enantiomeric amino acids between surface waters and the ocean's interior. *Limnol. Oceangr.* **48**, 755–763.

Radkov A. D. and Moe L. A. (2014) Bacterial synthesis of d-amino acids. *Appl. Microbiol. Biotechnol.* **98**, 5363–5374.

Repeta D. J. (2014) Chemical characterization and cycling of dissolved organic matter. In *Biogeochemistry of Marine Dissolved Organic Matter*. Academic Press, pp. 21–63.

Silfer J. A., Engel M. H., Macko S. A. and Jumeau E. J. (1991) Stable carbon isotope analysis of amino acid enantiomers by conventional isotope ratio mass spectrometry and combined gas chromatography/isotope ratio mass spectrometry. *Anal. Chem.* **63**, 370–374.

Simon M., Alldredge A. L. and Azam F. (1990) Bacterial carbon dynamics on marine snow. *Mar. Ecol. Prog. Ser.* **65**, 205–211.

Sipler R. E. and Bronk D. A. (2014) Dynamics of dissolved organic nitrogen. In *Biogeochemistry of Marine Dissolved Organic Matter*. Academic press, pp. 128–232.

Takano Y., Kashiyama Y., Ogawa N. O., Chikaraishi Y. and Ohkouchi N. (2010) Isolation and desalting with cation-exchange chromatography for compound-specific nitrogen isotope analysis of amino acids: application to biogeochemical samples. *Rapid Commun. Mass Spectrom.* **24**, 2317–2323.

Tremblay L. and Benner R. (2006) Microbial contributions to N-immobilization and organic matter preservation in decaying plant detritus. *Geochim. Cosmochim. Ac.* **70**, 133–146.

Walker B. D. and McCarthy M. D. (2012) Elemental and isotopic characterization of dissolved and particulate organic matter in a unique California upwelling system: Importance of size and composition in the export of labile material. *Limnol. Oceangr.* **57**, 1757.

Walker B. D., Beaupré S. R., Guilderson T. P., Druffel E. R. M. and McCarthy M. D. (2011) Large-volume ultrafiltration for the study of radiocarbon signatures and size vs. age relationships in marine dissolved organic matter. *Geochim. Cosmochim. Ac.* **75**, 5187–5202.

Walker B. D., Beaupré S. R., Guilderson T. P., McCarthy M. D. and Druffel E. R. M. (2016) Pacific carbon cycling constrained by organic matter size, age and composition relationships. *Nat. Geosci.*.

Walker B. D., Okimura K. M. and Guilderson T. P. (2014) Radiocarbon signatures and size–age–composition relationships of major organic matter pools within a unique California upwelling system. *Geochim. Cosmochim. Ac.* **126**, 1–17.

Williams P. M. and Druffel E. R. M. (1987) Radiocarbon in dissolved organic matter in the central North Pacific Ocean. *Nature* **330**, 246–248.

Woodward F. I. (2007) Global primary production. *Curr. Biol.* **17**, R269–R273.

Yamaguchi Y. T. and McCarthy M. D. (2018) Sources and transformation of dissolved and particulate organic nitrogen in the North Pacific Subtropical Gyre indicated by compound-specific δ15N analysis of amino acids. *Geochim. Cosmochim. Ac.* **220**, 329–347.

Yamashita Y. and Tanoue E. (2003) Distribution and alteration of amino acids in bulk DOM along a transect from bay to oceanic waters. *Mar. Chem.* **82**, 145–160.

Ziolkowski L. A. and Druffel E. R. M. (2010) Aged black carbon identified in marine dissolved organic carbon. *Geophys. Res. Lett.*, 37.

Associate editor: Jack J. Middelburg